Identification of protein-derived tyrosyl radical in the reaction of cytochrome *c* and hydrogen peroxide: characterization by ESR spin-trapping, HPLC and MS

Steven Yue QIAN*[1], Yeong-Renn CHEN*, Leesa J. DETERDING†, Yang C. FANN*, Colin F. CHIGNELL*, Kenneth B. TOMER† and Ronald P. MASON*

*Laboratory of Pharmacology and Chemistry, National Institute of Environmental Health Sciences, National Institutes of Health, P.O. Box 12233, Research Triangle Park, NC 27709, U.S.A., and †Laboratory of Structural Biology, National Institute of Environmental Health Sciences, National Institutes of Health, P.O. Box 12233, Research Triangle Park, NC 27709, U.S.A.

The reaction of cytochrome *c* and H_2O_2 is known to form a protein-centred radical that can be detected with the spin trap 2-methyl-2-nitrosopropane (MNP). To characterize the MNP/tyrosyl adduct structure that had previously been determined incorrectly [Barr, Gunther, Deterding, Tomer and Mason (1996) J. Biol. Chem. **271**, 15498–15503], we eliminated unreasonable structure models by ESR studies with a series of ^{13}C-labelled tyrosines, and photochemically synthesized an authentic MNP/tyrosyl adduct that has its trapping site on the C-3 position of the tyrosine phenyl ring. The observation of the identical ESR spectra for this radical adduct from the UV irradiation of 3-iodo-tyrosine and the adduct from the cytochrome *c* reaction demonstrated that the radical trapping site of MNP/tyrosyl is located on the equivalent C-3/C-5 positions instead of the C-1 position, as was proposed by Barr et al. In an on-line HPLC/ESR system, an identical retention time (17.7 min) was observed for the ESR-active HPLC peak of the MNP/tyrosyl adduct from the following three reactions: (i) the tyrosine oxidation via horseradish peroxidase/H_2O_2; (ii) UV irradiation of 3-iodo-tyrosine and (iii) the reaction of cytochrome *c* with H_2O_2. This result demonstrated that the radical adducts of all three reactions are most probably the same. The mass spectrometric analysis of the HPLC fractions from reactions (i) and (ii) showed an ion at *m/z* 267 attributed to the MNP/tyrosyl adduct. We conclude that the cytochrome *c*-derived tyrosyl radical was trapped by MNP, leading to a persistent radical adduct at the C-3/C-5 positions of the tyrosine phenyl ring.

Key words: ESI mass spectrometry, on-line HPLC/ESR, radical identification, tandem mass spectrometry.

INTRODUCTION

In most aerobic mammalian cells, mitochondria represent a primary source of reactive oxygen species [1–5]. Oxidative stress in mitochondria is a possible cause of many human diseases, including heart disease, aging and cancer, and has attracted much attention for several decades [6–11]. Mitochondria, especially mitochondrial membranes, are continuously challenged by oxidative stress because mitochondria not only generate superoxide ($O_2^{\cdot-}$) and H_2O_2, but also contain high concentrations of non-haem and haem protein-bound iron that can serve as strong oxidants via their reactions with H_2O_2. One such haem protein is cytochrome *c*, which can react with H_2O_2 to form a highly reactive ferryl-haem species capable of oxidizing various organic molecules and initiating lipid peroxidation [12–16].

When cytochrome *c* reacts with H_2O_2, it forms a protein-derived tyrosyl radical. This radical, trapped by 2-methyl-2-nitrosopropane (MNP), was first observed with the ESR spin-trapping technique by Barr et al. [17]. At the time, the radical-trapping site was assigned to the C-1 position of the tyrosine phenyl ring which, by hydrogen bonding, could then form an additional seven-member ring (Scheme 1) [17,18]. However, a recent NMR study [19] on the generation of myoglobin-derived tyrosyl radical from the reaction of myoglobin and H_2O_2 suggested that the more probable trapping site might be the equivalent C-3/C-5 positions.

The determination of radical structure via the ESR spin-trapping technique is based on the hyperfine couplings of the ESR spectra. However, whereas the ESR hyperfine couplings can provide detailed information about the radical centre, they do not provide comprehensive structural information such as the

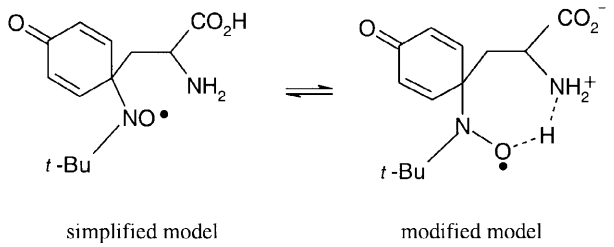

Scheme 1 Proposed C-1 structure of the MNP/tyrosyl adduct

t-Bu, t-butyl.

Abbreviations used: ESI, electrospray ionization; HRP, horseradish peroxidase; MNP, 2-methyl-2-nitrosopropane; MNP-d_9, 2-methyl (deuterium)-2-nitrosopropane; MS/MS, tandem MS; t_R, retention time; a^N, nitrogen hyperfine coupling; a^H, hydrogen hyperfine coupling.

[1] To whom correspondence should be addressed (e-mail qian1@niehs.nih.gov).

molecular mass of the radical adduct, nor can they distinguish between alternative structures predicted to have similar coupling constants. Thus in order to resolve the question of where the tyrosyl radical is trapped, further structural information is needed.

In the present study, we have determined the structure of the MNP/tyrosyl adduct formed from the reaction of cytochrome *c* with H_2O_2 in the presence of MNP using a variety of approaches and techniques. We eliminated unreasonable structural models by using ESR spin-trapping methods to examine a series of ^{13}C-labelled tyrosines oxidized by horseradish peroxidase (HRP)/H_2O_2. To provide a standard, we photochemically synthesized an authentic MNP/tyrosyl adduct with the C-3 position as the radical-trapping site [20]. The ESR results of the photochemical synthesis were consistent with the ^{13}C-labelled ESR results, demonstrating that the trapping site of the MNP/tyrosyl adduct in these models is not the C-1 position, but rather the C-3/C-5 positions.

To further characterize the structure of the MNP/tyrosyl adduct, we combined ESR spin trapping with HPLC and MS. On-line HPLC/ESR [21–23], a technique to detect ESR-active peaks in the HPLC elution profile, allowed us to test the structural similarities of various adducts. Combining HPLC/ESR with MS analysis has allowed us to determine the molecular mass of a variety of radical adducts [24–28]. Using this combined technique, we have successfully characterized the MNP/tyrosyl radical adduct generated in three independent ways: from UV irradiation of 3-iodo-tyrosine, from tyrosine oxidation via HRP/H_2O_2 and from the reaction of cytochrome *c* with H_2O_2. We conclude that the oxidation of cytochrome *c* with H_2O_2 forms a cytochrome *c*-derived tyrosyl radical that is trapped by MNP at the C-3/C-5 positions of the tyrosine phenyl ring.

EXPERIMENTAL

Reagents

Horse heart cytochrome *c*, HRP type VI-A, L-tyrosine and 1.0 M HCl were purchased from Sigma (St. Louis, MO, U.S.A.). The concentrations of horse heart cytochrome *c* and HRP were verified with UV absorption at 550 nm ($\epsilon \approx 18.5\ mM^{-1} \cdot cm^{-1}$) and 402 nm ($\epsilon \approx 102\ mM^{-1} \cdot cm^{-1}$), respectively. The ^{13}C-labelled tyrosines, L-4-hydroxyphenyl-$^{13}C_6$-alanine, L-4-hydroxyphenyl-alanine-3′-^{13}C and L-4-hydroxyphenylalanine-4-^{13}C were purchased from Cambridge Isotope Laboratory (Andover, MA, U.S.A.). The 3-iodo-tyrosine and the spin trap MNP were obtained from Aldrich (Milwaukee, WI, U.S.A.). H_2O_2 was purchased from Fisher (St. Louis, MO, U.S.A.), and its concentration was verified with UV absorption at 240 nm ($\epsilon \approx 43.6\ M^{-1} \cdot cm^{-1}$). Perdeuterated MNP-$d_9$ [2-methyl (deuterium)-2-nitrosopropane] was provided as a gift from Dr J. Joseph (Medical College of Wisconsin, Milwaukee, WI, U.S.A.). Pronase was purchased from Boehringer Mannheim. Prepacked Sephadex G-25 (PD-10) size-exclusion cartridges were purchased from Pharmacia Biotech (Uppsala, Sweden). All experiments were performed in 50 mM potassium phosphate-buffered aqueous solution (pH 7.4), except for the photochemical experiment, which was performed in HCl aqueous solution at low pH (pH 1.3) or deionized water.

ESR measurement

ESR spectra were obtained with a Bruker ElexSys E500 spectrometer equipped with a super-high Q cavity operating at 9.77 GHz and room temperature. The ESR spectrometer settings were: modulation frequency, 100 kHz; modulation amplitude, 0.2–4.0 G; microwave power, 20 mW; receiver gain, 10^5–10^6 and time constant, 0.6–2.0 s. ESR computer simulation was accomplished using software developed in this laboratory [29].

Spin-trapping of the protein-derived and UV-derived radicals

In order to achieve the optimum ESR signal for the protein-derived radical adduct, the mixture of reactants was allowed to react for 10–30 min and then loaded into a Sephadex G-25 size-exclusion column. The sample was passed through the exclusion column by eluting with 50 mM phosphate buffer (pH 7.4), thus removing excess H_2O_2, free MNP and non-protein spin adducts from the protein-bound fraction. The protein portion was collected and subjected to 20 min of non-specific proteolysis by Pronase, after which HPLC separation and ESR measurements were performed.

To synthesize the MNP/tyrosyl adduct known to be trapped at the C-3 site, we dissolved 3-iodo-tyrosine in HCl aqueous solution. At room temperature and with the presence of MNP, the iodo-tyrosine solution was irradiated for 5 min under UV light from a high-pressure mercury lamp (1000 W) equipped with a water filter.

On-line HPLC/ESR

An on-line HPLC/ESR system was used to detect and separate the MNP/tyrosyl adduct formed in the following reactions: tyrosine oxidation via HRP/H_2O_2, UV irradiation of 3-iodo-tyrosine and the reaction of cytochrome *c* with H_2O_2. The on-line HPLC/ESR system consisted of a Hewlett–Packard 1100 series HPLC system and a Bruker ElexSys spectrometer. The outlet of the Waters UV detector was connected to the ESR AquaX cell with Red Peek HPLC tubing (0.127 mm internal diameter). In addition, in this system two ESR settings were increased in order to heighten sensitivity: modulation amplitude (4.0 G) and time constant (2.0 s).

In the on-line system, HPLC separations were performed on a C_{18} column (Hewlett Packard Zorbax; 4.6 mm × 250 mm) equilibrated with solvent A (10 mM ammonium acetate). The reaction mixture (50–500 μl) was typically injected into the HPLC column and eluted at a 1.0 ml/min flow rate for 50 min with a gradient of 0–75 % solvent B (10 mM ammonium acetate/80 % acetonitrile). We monitored the UV absorption at 280 nm and the ESR signal with a magnetic field fixed on the middle line of the ESR triplet for the MNP radical adducts. The peaks with corresponding absorptions in both the UV trace and the ESR trace were collected according to their HPLC retention time, lyophilized and subjected to mass spectrometric analysis.

Electrospray ionization (ESI) MS

ESI mass spectra were acquired with a Micromass Q-Tof (Altrincham, Cheshire, U.K.) hybrid tandem mass spectrometer [30]. ESI-MS conditions were as follows: needle voltage, ≈ 3000 V; cone voltage, 25 V; collision energy, 4.0 eV; source temperature, 80 °C; sample infusion, ≈ 200 nl/min using a pressure-injection vessel [31] and data-acquisition range, m/z 50–3000 at 1.9 s/scan. For the tandem MS (MS/MS) experiments, a parent ion was selected with the first mass analyser and transmitted into a collision cell where fragmentation was induced by collision with argon atoms at a collision energy of 25 eV. The resulting fragment ions were detected with the second mass analyser. In this type of experiment, only ions resulting from fragmentation of the selected parent ion were observed. Data analysis was accomplished with a MassLynx data system and MaxEnt software supplied by the manufacturer.

RESULTS

ESR spin trapping of cytochrome *c*-derived tyrosyl radical

When cytochrome *c* (500 μM) was allowed to react with 2.5 mM H_2O_2 in the presence of MNP, an ESR spectrum (Figure 1A) was detected. This spectrum was composed of a trace of di-t-butylnitroxide ($a^N = 17.1$ G [32], where a^N is the nitrogen hyperfine coupling; marked as * in Figure 1A) and an immobilized nitroxide derived from MNP trapping of a protein-centred radical. After the solution was passed through a size-exclusion chromatographic column, only the protein-bound adduct was detected in the protein fraction (Figure 1B). When this protein-derived adduct was subjected to non-specific proteolysis by the addition of 2 mg/ml Pronase, a three-line spectrum was detected with a hyperfine coupling of 15.5 G (Figure 1C). Because an identical ESR spectrum (Figure 1D), previously identified as the MNP/tyrosyl adduct [17], can be detected from tyrosine oxidation via HRP/H_2O_2 or myeloperoxidase/H_2O_2 [33], the protein-bound adduct was assigned as a protein-derived tyrosyl radical.

ESR spin trapping of MNP/tyrosyl adducts from ^{13}C-labelling experiments

The three-line spectrum of the MNP/tyrosyl adduct suggested that the radical might be trapped on the tertiary carbon atom of tyrosine, i.e. in the C-1 position, because none of the neighbouring atoms (β-position) has a nuclear spin. A β-hydrogen or a β-nitrogen in the MNP adduct would give rise to small hyperfine coupling constants in addition to the large nitrogen splitting visible in Figure 1(D). Originally, it seemed likely that the tyrosyl radical had been trapped at the C-1 position because the spin density is highest at that position [34]. On the basis of a molecular model calculation, a modified C-1 model was proposed [18] as the structure of the MNP/tyrosyl adduct with hydrogen bonding forming an additional seven-member ring (Scheme 1). In a recent NMR study on the reaction of myoglobin and H_2O_2 [19], however, the C-3/C-5 trapping site was proposed because the three hydrogen hyperfine couplings in MNP-tyrosyl were observed to be aromatic.

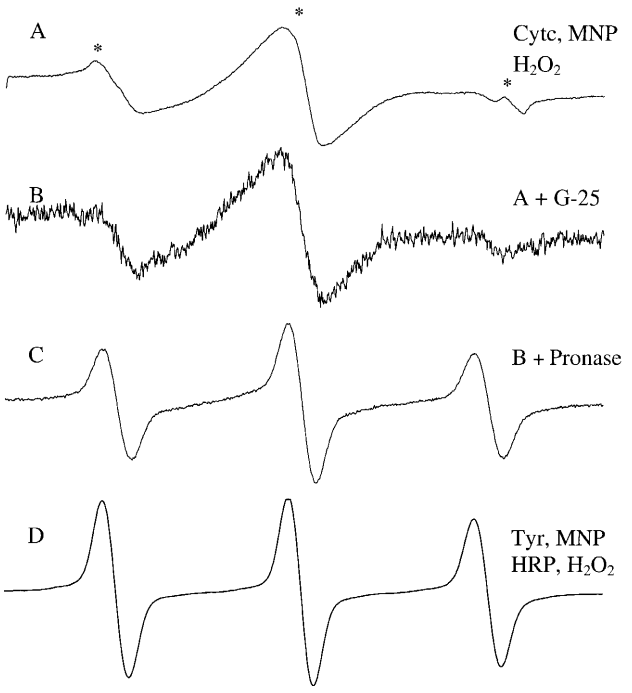

Figure 1 ESR spectra of the MNP/tyrosyl radical adduct obtained from enzymic oxidation

(**A**) The reaction mixture contained 500 μM cytochrome *c* (Cytc), 2.5 mM H_2O_2 and 21 mM MNP. The ESR spectrum was collected 30 min after addition of the last reagent, H_2O_2. (**B**) Sample A was loaded into a Sephadex G-25 size-exclusion column and eluted with 50 mM sodium phosphate buffer (pH 7.4). About one-quarter of the protein-bound eluate was used for this ESR measurement. (**C**) Sample B was treated with 2 mg/ml Pronase. (**D**) The reaction mixture contained 2 mM tyrosine, 1.0 mM H_2O_2, 2.5 μM HRP and 21 mM MNP. The ESR spectrum was collected 10 min after the last reagent, H_2O_2, was added. The ESR settings were: microwave power, 20 mW; modulation amplitude, 1 G; time constant, 0.65 s; scan time, 335 s; receiver gain, 2.5×10^5 and sweep width, 50 G.

In order to distinguish between the C-1 and C-3/C-5 structures and to rule out other trapping positions, we performed ESR spin trapping with a series of ^{13}C-labelled tyrosines. Hyperfine coupling constants from ^{13}C located on either the α-position or the β-position neighbouring the radical centre of an MNP adduct are generally large enough to resolve. To test these structures, we chose three ^{13}C-labelled tyrosines: L-4-hydroxyphenyl-$^{13}C_6$-alanine, L-4-hydroxyphenylalanine-3′-^{13}C and L-4-hydroxyphenylalanine-4-^{13}C.

All carbons in the phenyl ring of L-4-hydroxyphenyl-$^{13}C_6$-alanine were labelled with ^{13}C; therefore, we expected to see multiple ^{13}C splittings if the tyrosyl radical were trapped at any position on the phenyl ring. The three-line spectrum detected from the ^{12}C tyrosine oxidation (Figure 2A) was replaced by an eight-line spectrum (Figure 2B) composed of hyperfine couplings from nitrogen ($a^N = 15.5$ G), one α-^{13}C ($a^{13C} = 7.1$ G) and two apparently equivalent β-^{13}C atoms ($a^{13C} = 8.0$ G). Both α- and β-^{13}C hyperfine coupling constants should be large enough to resolve [17,32]. The dotted lines in Figure 2(B) represent the computer simulations, but no additional hyperfine coupling (1.3 G [33]) could be resolved. When MNP-d_9 was used instead of MNP in the oxidation of L-4-hydroxyphenyl-$^{13}C_6$-alanine, an additional ^{13}C hyperfine coupling was clearly resolved, $a^{13C} =$ 0.6 G (results not shown). This result demonstrated that the trapping site of the MNP/tyrosyl adduct was located on the phenyl ring of tyrosine, but did not specify which phenyl carbon was the trapping site.

In a previous ESR spin-trapping study, we eliminated the possibility of the C-4 (or O) atoms as the trapping site by replacing the phenolic oxygen ^{16}O in tyrosine with ^{17}O [18]. Based on the known positions of high spin density [34], the other possible positions on the tyrosyl phenyl ring for the radical-trapping site should be the C-1 and the equivalent C-3/C-5 positions.

To test the possibility of C-1 as the radical-trapping site, we performed a spin-trapping experiment with L-4-hydroxyphenylalanine-3′-^{13}C oxidation via HRP/H_2O_2. If the radical-trapping site of MNP/tyrosyl adduct were located on the C-1 position, the nuclear spin of ^{13}C of L-4-hydroxyphenylalanine-3′-^{13}C would be located in the β-position relative to the radical centre and would contribute a hyperfine coupling to give a six-line ESR spectra (a triplet for nitrogen, and a further split by doublet ^{13}C at the β-position). However, only a three-line ESR spectrum was observed for this compound (Figure 2C), indicating that the ^{13}C was not located on the β-position.

To test for the trapping site at the C-3/C-5 positions, L-4-hydroxyphenylalanine-4-^{13}C was oxidized with HRP/H_2O_2. If either the C-3 or the C-5 position were the trapping site, ^{13}C would be the β-carbon neighbouring the radical centre of the MNP/tyrosyl adduct and would contribute to its hyperfine coupling pattern. The observation of a six-line spectrum (Figure 2D) composed of a coupling from nitrogen ($a^N = 15.5$ G) and a

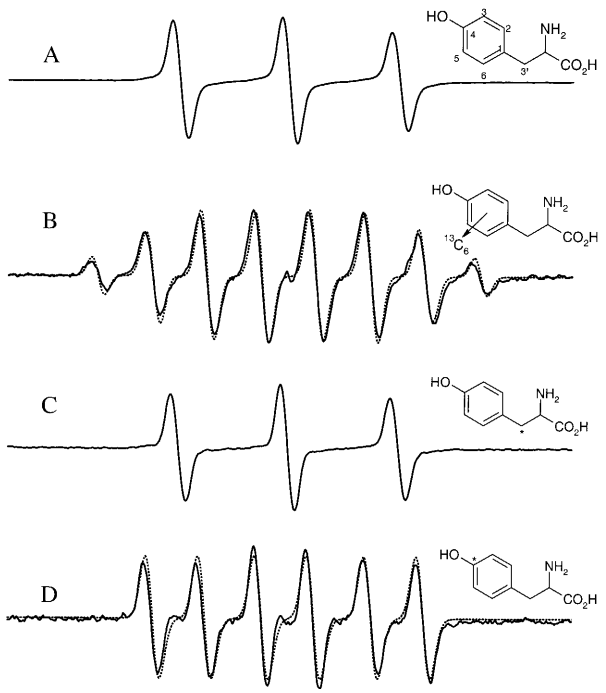

Figure 2 ESR spectrum of the MNP/tyrosyl radical adduct obtained from the oxidation of tyrosine and ^{13}C-labelled tyrosines by HRP and H_2O_2

The reaction mixture was the same as in Figure 1D, except that the isotopically labelled tyrosines L-4-hydroxyphenylalanine-3′-^{13}C, L-4-hydroxyphenyl-$^{13}C_6$-alanine and L-4-hydroxyphenylalanine-4-^{13}C were used instead of tyrosine. The solid lines are the experimental ESR spectra; the dotted lines are the computer simulations. Different ESR collection times were used for each experiment to obtain the optimum ESR signal. Shown are the MNP/tyrosyl adducts from (**A**) $^{12}C_6$-tyrosine, (**B**) L-4-hydroxyphenyl-$^{13}C_6$-alanine, (**C**) L-4-hydroxyphenylalanine-3′-^{13}C and (**D**) L-4-hydroxyphenylalanine-4-^{13}C. The ESR settings were: microwave power, 20 mW; modulation amplitude, 0.5 G; time constant, 0.65 s; scan time, 335 s; receiver gain, 2.5×10^5 and sweep width, 80 G. * indicates the ^{13}C position.

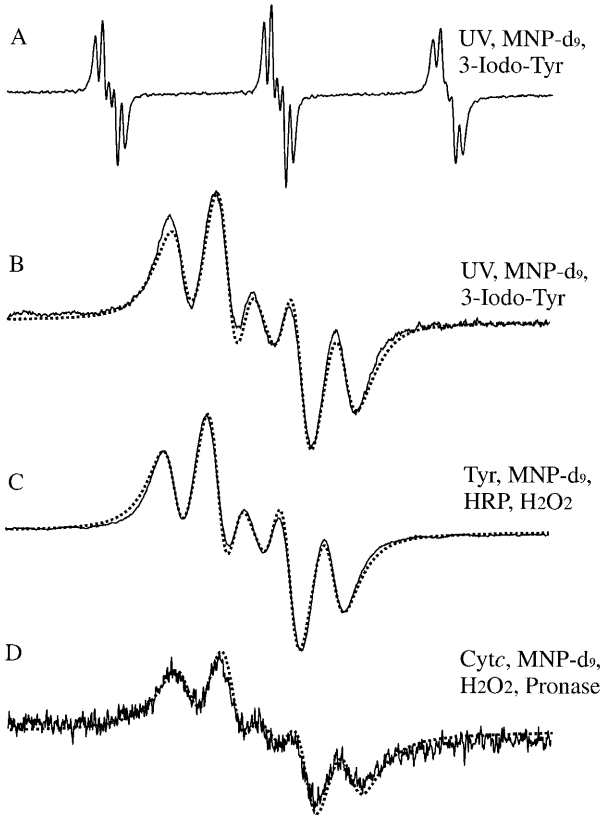

Figure 3 ESR spectra of MNP-d_9/tyrosyl radical adducts obtained from various reactions

Spectrum (**A**) was obtained with a 50 G sweep of the entire ESR spectrum of the MNP-d_9/tyrosyl radical adduct, whereas spectra (**B**)–(**D**) were obtained with an 8 G sweep, accenting the super-hyperfine structure of the middle line of the primary triplet of MNP-d_9 adducts. The solid lines represent the experimental ESR spectra from the experiments; the dotted lines represent the computer simulations. The ESR spectra were obtained 10 min after addition of H_2O_2. (**A**) The reaction mixture contained 2 mM 3-iodo-tyrosine (3-Iodo-Tyr) in water and 21 mM MNP. The ESR spectrum was measured after 5 min of UV irradiation. (**B**) Same as (**A**), but with an 8 G sweep. (**C**) The reaction mixture contained 2 mM tyrosine, 1.0 mM H_2O_2, 2.5 μM HRP and 21 mM MNP-d_9. (**D**) The reaction mixture contained 500 μM cytochrome *c* (Cyt*c*), 2.5 mM H_2O_2 and 21 mM MNP-d_9. The reaction was allowed to proceed for 30 min, loaded into a Sephadex G-25 size-exclusion column and eluted with 50 mM sodium phosphate buffer (pH 7.4). About one-quarter of the protein-bound eluate (200 μl) was mixed with 2 mg/ml Pronase before ESR measurement. The ESR settings were: microwave power, 20 mW; modulation amplitude, 0.2 G; time constant, 0.65 s; scan time, 335 s and receiver gain, 2.5×10^5.

β-^{13}C ($a^{13C} = 7.4$ G) clearly supports the C-3/C-5 position as the trapping site of the MNP/tyrosyl radical adduct.

ESR spin trapping of the authentic MNP/tyrosyl adduct

To further confirm the C-3/C-5 structure as the trapping site of the MNP/tyrosyl radical adduct, we photochemically synthesized an authentic MNP/tyrosyl radical adduct by UV irradiation of 3-iodo-tyrosine in the presence of MNP-d_9 (i.e. with the nine methyl hydrogens replaced by deuterium) [20] (see Scheme 2).

Deuteration of MNP decreased the broadening effect on the hyperfine structure of the nine methyl hydrogens, thereby enhancing the resolution of the smaller hyperfine coupling constants of MNP radical adducts. In Scheme 2, it is known that the radical is trapped at the C-3 position of the tyrosine phenyl ring; its ESR spectrum (Figures 3A and 3B) consisted of hydrogen hyperfine couplings (a^H) of $a^H = 1.06$ G, $a^H = 0.69$ G and $a^H = 0.64$ G, as shown by its computer simulation (Figure 3, dotted

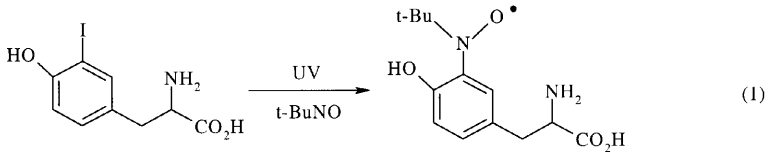

(1)

Scheme 2 Photochemical synthesis of authentic MNP/tyrosyl adducts

lines). The better resolution of the super-hyperfine couplings of this adduct was obtained with an 8 G scan (Figure 3B) of the centre-field line of the primary triplet seen in the 50 G scan in Figure 3(A). The splittings of Figure 3(B) are comparable with those reported by Gunther et al. [18] of one non-equivalent hydrogen coupling ($a^H = 1.05$ G) and two nearly equivalent hydrogen atoms ($a^H = 0.7$ and 0.55 G).

We further used MNP-d_9 to trap the tyrosyl radical generated in our experimental systems. In the presence of perdeuterated MNP, we obtained identical multi-line ESR spectra from the oxidation of tyrosine by HRP/H_2O_2 (Figure 3C) and the reaction of cytochrome *c* with H_2O_2, but with lower intensity (Figure 3D). These high-resolution ESR spectra shown as its computer simulation (Figure 3D, dotted line) consisted of hydrogen hyperfine couplings that were identical to those in Figure 3(B).

On-line HPLC/ESR study

To further confirm that the MNP/tyrosyl adducts derived from the three different reactions were identical, we combined ESR and HPLC with an on-line system to separate both the ESR-active radical adducts and the non-ESR-active species. For the UV irradiation of 3-iodo-tyrosine, the peak with a retention time, t_R, of 17.7 min was attributed to the MNP/tyrosyl adducts because it exhibited absorption in both the UV trace (280 nm) and the ESR trace (the peak of the middle line of the ESR spectrum). When this HPLC fraction was collected and subjected to ESR spectroscopy, the ESR super-hyperfine couplings observed were essentially identical to those seen in Figure 2(A) (results not shown), thus confirming the assignment.

We found that the ESR-active HPLC fractions in all three reactions, i.e. UV-irradiated 3-iodo-tyrosine (Figure 4A), the oxidation of tyrosine by HRP/H_2O_2 (Figure 4B) and the reaction of cytochrome *c* with H_2O_2 (Figure 4C), had identical t_R values of 17.7 min. The strongest ESR-active HPLC peak was observed in the UV irradiation of the 3-iodo-tyrosine system, whereas a weaker ESR absorption was found in the HRP/H_2O_2/tyrosine system. In the cytochrome *c* oxidation system, however, at 17.7 min the UV absorption signal was only a little higher than that of the background level (Figure 4C, *), and the on-line ESR signal was undetectable. To obtain a detectable ESR signal from the reaction of cytochrome *c* and H_2O_2, we collected and measured the 17.7 min HPLC fraction via off-line ESR. Unlike on-line ESR, off-line ESR can be enhanced via a signal-averaging technique. A 25-scan accumulated spectrum in off-line ESR indicated a clear multi-line ESR spectrum of the MNP-d_9/tyrosyl adduct (Figure 4C, inset).

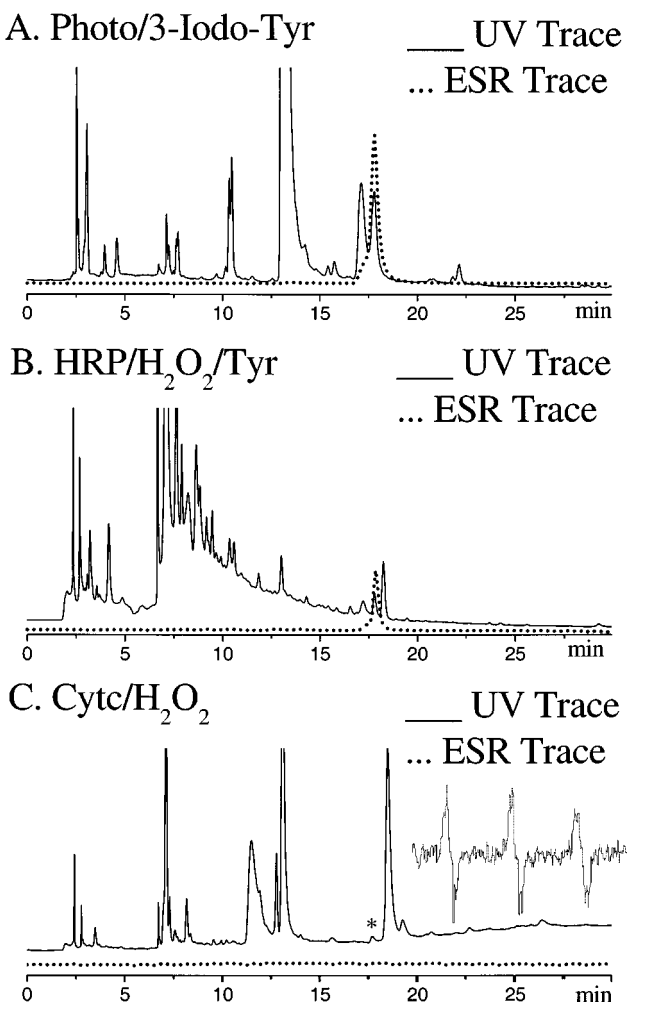

Figure 4 HPLC/ESR on-line analysis of MNP/tyrosyl radical adduct from various reactions

The MNP/tyrosyl adducts were monitored by UV absorption at 280 nm (solid lines) and ESR (dotted lines). (**A**) UV and ESR traces were obtained from the reaction mixture of 3-iodo-tyrosine that was UV-irradiated in the presence of MNP. (**B**) UV and ESR traces were obtained from tyrosine oxidized by HRP and H_2O_2 in the presence of MNP. (**C**) UV and ESR traces were obtained after Pronase treatment of the protein-bound radical adduct from the reaction of cytochrome *c* with H_2O_2.

MS of MNP adducts

To further characterize the structure of the MNP/tyrosyl radical adduct, the ESR-active HPLC fraction ($t_R = 17.7$ min) from all three reactions was analysed by ESI-MS. To aid in the MS identification of ions associated with the MNP/tyrosyl adduct, a dual spin-trapping technique was utilized with the model system (i.e. UV irradiation of 3-iodo-tyrosine). In dual spin-trapping experiments, a 50:50 mixture of MNP/MNP-d_9 spin traps is used instead of MNP or MNP-d_9 alone. As a result, ion pairs with a difference of 9 mass units (m/z 267 and m/z 276) are observed in the mass spectra (Figure 5A), corresponding to the oxidized forms of MNP/tyrosyl and MNP-d_9/tyrosyl adducts, respectively (Scheme 3).

To confirm the identity of these ions, the MS/MS spectra of m/z 267 and m/z 276 were acquired (Figures 5B and 5C, respectively) and showed similar fragment ions. The ions of m/z 92 and m/z 120 were observed in both spectra and correspond to C_7H_8 and C_8H_8O, respectively. In addition, the loss of C_4H_8 (or $C_4{}^2H_8$) from m/z 267 (or m/z 276) was observed at m/z 211 (Figure 5B) and m/z 212 (Figure 5C), respectively, corresponding to the loss of the t-butyl group of MNP. Cleavage of both the t-butyl and N-OH groups from MNP resulted in the fragment ion at m/z 179 (Figures 5B and 5C). These data confirm that the pair of ions of m/z 267 and m/z 276 are the MNP/tyrosyl and MNP-d_9/tyrosyl adducts.

The ESI mass spectrum from the HRP/H_2O_2 system showed both ions of oxidized form (m/z 267) and reduced form (m/z 269) of the MNP/tyrosyl adduct (Scheme 3). The MS/MS spectrum of m/z 267 (Figure 5D) showed a similar fragmentation pattern to that observed in the MS/MS spectrum of the ion of m/z 267 from the MNP model system (Figure 5B). These results demonstrate clearly that the MNP/tyrosyl adduct formed from tyrosine oxidation by HRP/H_2O_2 is identical to that formed from the UV irradiation of 3-iodo-tyrosine. The concentration of

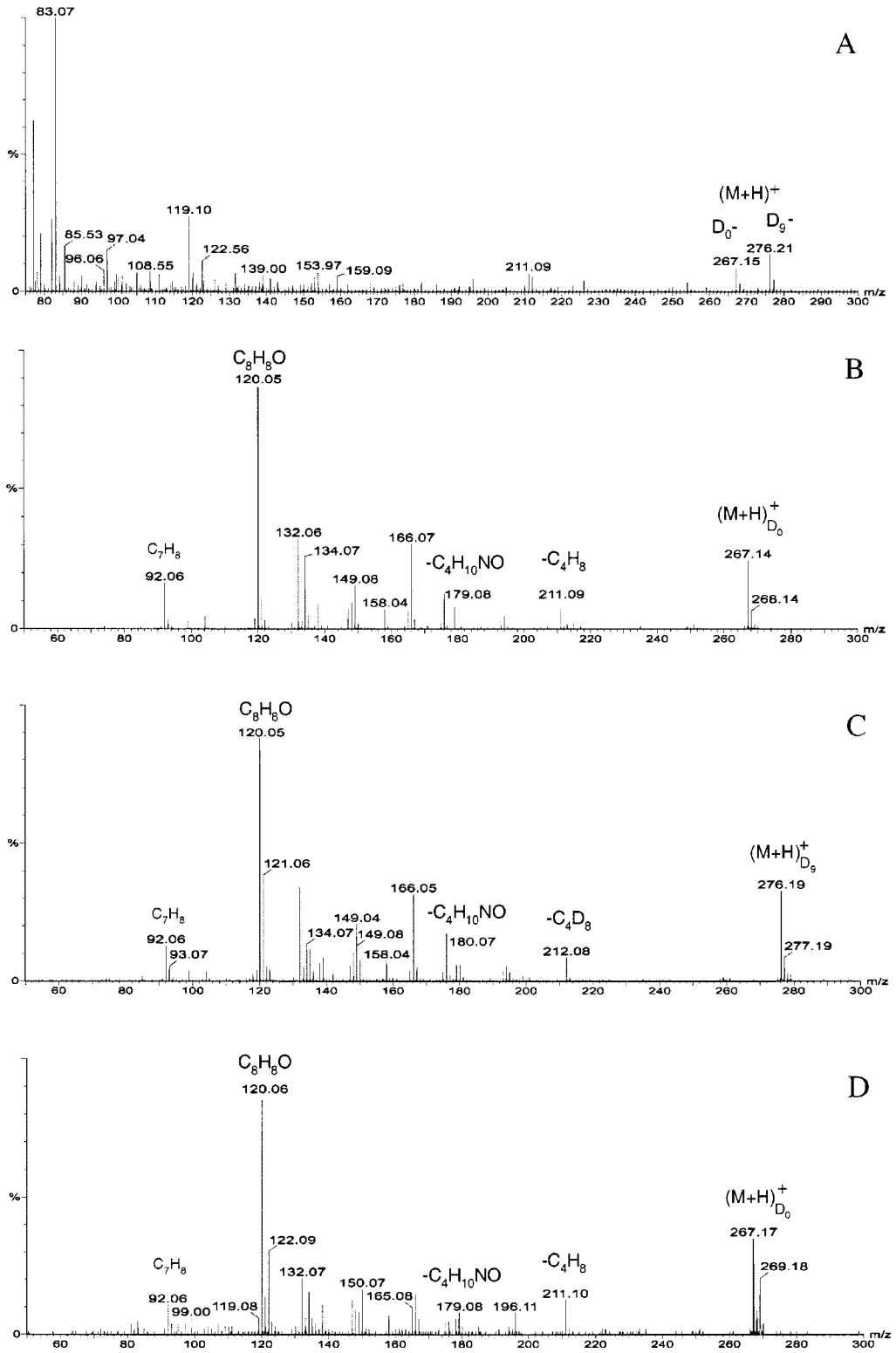

Figure 5 Mass spectra of the ESR-active HPLC fractions from the UV-irradiated 3-iodo-tyrosine system using a 50:50 mixture of MNP/MNP-d_9 spin trap

(**A**) Full-scan mass spectrum of the ESR-active HPLC fraction, (**B**) MS/MS spectrum of the $(M+H)^+$ ion of *m/z* 267, (**C**) MS/MS spectrum of the $(M+H)^+$ ion of *m/z* 276 and (**D**) MS/MS spectrum of the $(M+H)^+$ ion of *m/z* 267 from HRP/H_2O_2-oxidized tyrosine in the presence of MNP.

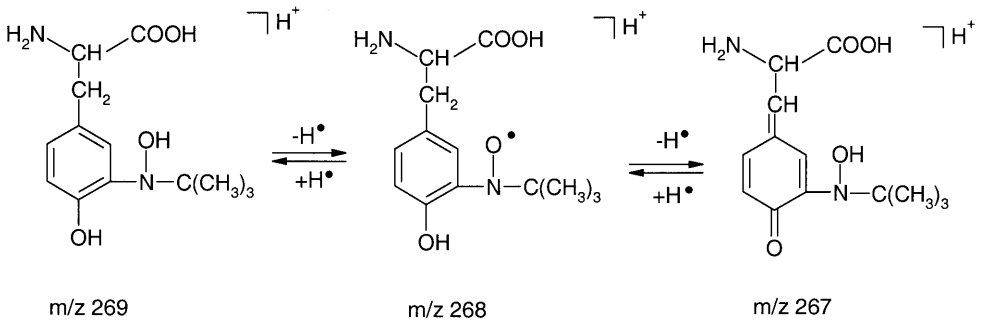

Scheme 3 Molecular ions of the MNP/tyrosyl adduct and its reduced and oxidized forms

the MNP/tyrosyl adduct formed via the third system, cytochrome *c* oxidation, was too low to be detected by MS analysis.

DISCUSSION

Characterization of the structure of the MNP/tyrosyl radical adduct has important implications in the mechanism of radical generation since protein-derived tyrosyl radicals are formed as catalytic intermediates in enzymes and as the result of oxidative stress. We have successfully performed ESR spin-trapping studies in different tyrosyl-radical-generating systems, including UV irradiation of 3-iodo-tyrosine and a series of ^{13}C-labelled MNP/tyrosyl radical adducts formed by oxidation with HRP/H_2O_2, to confirm that the equivalent C-3/C-5 positions are the trapping sites of the MNP/tyrosyl radical adduct formed in the HRP/H_2O_2 system. Steric hinderance may lead to a preference for one of the C-3/C-5 positions in the formation of the MNP/tyrosyl radical adduct in the cytochrome *c* and H_2O_2 system. With proteolysis of the cytochrome *c* radical adduct, any evidence for preferential binding of one of the C-3/C-5 positions would be lost. With on-line HPLC/ESR analysis, the MNP/tyrosyl adducts from all three reaction systems, UV irradiation of 3-iodo-tyrosine, HRP/H_2O_2 oxidizing tyrosine and cytochrome *c* oxidized by H_2O_2, were confirmed to form the same MNP/tyrosyl adduct, with the C-3/C-5 positions as the radical-trapping site. Using a double spin-trapping experiment and MS analysis, ions of *m/z* 267 and *m/z* 276 were identified to be MNP/tyrosyl and MNP-d_9/tyrosyl adducts formed either by UV irradiation of 3-iodo-tyrosine or HRP/H_2O_2 oxidation of tyrosine. These data allow unambiguous determination of the MNP/tyrosyl radical adduct formed from all three different reactions to be trapped by MNP at the C-3/C-5 positions of the tyrosine phenyl ring.

Based on a molecular conformation calculation and ESR analysis, the C-1 model was originally proposed as the radical-trapping site of MNP/tyrosyl radical adduct, with an additional seven-membered ring formed by hydrogen bonding [17]. The tertiary carbon of the phenyl ring was proposed as the trapping site, mainly because no β–H hyperfine couplings were observed by ESR for the MNP adduct. If the radical-trapping site were located on other carbons in the phenyl ring, such as the C-3/C-5 positions (Scheme 4), the observation of β–H hyperfine couplings in the ESR spectrum would be expected. The absence of β–H hyperfine couplings, however, could also result from the fast rearrangement of the radical adduct with loss of the β–H to form an aromatic nitroxide [35,36]. In this study, the ESR hyperfine structure of the MNP/tyrosyl adduct was determined by using isotopically substituted MNP-d_9 as a spin trap. This

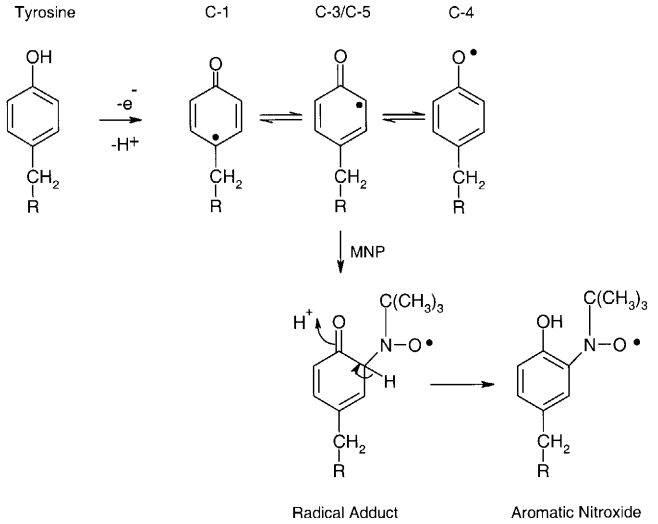

Scheme 4 The proposed spin-trapping mechanism of the tyrosyl radical

result revealed three small ring hydrogen couplings in addition to the large nitrogen coupling observed with MNP, as reported by Gunther et al. [18]. When MNP traps an aryl radical that has an *ortho* substituent, the ESR spectra shows an increase in a^N of the nitroxide group and a decrease in a^H of the ring protons. This is because the nitroxide group of the resultant adduct is rotated out of the plane of the aromatic ring, thereby decreasing conjugation between the nitroxide moiety and the phenyl ring [37,38].

In order to determine the trapping site unambiguously, ESR spin trapping, HPLC and MS analysis were used to ascertain the structure of MNP/tyrosyl adducts formed from three systems: UV irradiation of 3-iodo-tyrosine, tyrosine oxidation by HRP/H_2O_2 and cytochrome *c* oxidation via H_2O_2. The MNP/tyrosyl radical adduct was trapped unambiguously at the C-3 position by UV irradiation of 3-iodo-tyrosine.

In the on-line HPLC/ESR experiments, ESR-active fractions from all three reactions gave identical t_R values (17.7 min), indicating that the MNP/tyrosyl adducts formed from these reactions have identical structures. This was confirmed further with a series of ^{13}C-labelled tyrosine experiments in which the results were consistent with trapping at the C-3/C-5 positions, not the C-1 position. Although isotope labelling is a powerful

tool in ESR spectroscopy for the characterization of radical structures, it does not generally provide comprehensive structural determination. For example, the molecular mass of the radical adduct cannot be determined, and the lack of such comprehensive structural information is a major weakness in the determination of radical adduct structures by ESR alone.

MS analysis of the adducts was used to verify the structure of the MNP/tyrosyl adduct. A 50:50 mixture of MNP and MNP-d_9 was used to help identification of the ions associated with the MNP/tyrosyl radical adduct. MS/MS analysis of these ions showed unambiguously that their structures were consistent with the MNP/tyrosyl and MNP-d_9/tyrosyl adducts.

We are grateful to Ms Mary Mason and Dr Ann Motten for their help in editing the manuscript.

REFERENCES

1 Boveris, A., Oshino, N. and Chance, B. (1972) The cellular production of hydrogen peroxide. Biochem. J. **128**, 617–630
2 Boveris, A. and Chance, B. (1973) The mitochondrial generation of hydrogen peroxide. Biochem. J. **134**, 707–716
3 Boveris, A., Cadenas, E. and Stoppani, A. O. M. (1976) Role of ubiquinone in the mitochondrial generation of hydrogen peroxide. Biochem. J. **156**, 435–444
4 Turrens, J. F. and Boveris, A. (1980) Generation of superoxide anion by the NADH dehydrogenase of bovine heart mitochondria. Biochem. J. **191**, 421–427
5 Turrens, J. F., Alexandre, A. and Lehninger, A. L. (1985) Ubisemiquinone is the electron-donor for superoxide formation by complex III of heart mitochondria. Arch. Biochem. Biophys. **237**, 408–414
6 Darley-Usmar, V. and Halliwell, B. (1996) Blood radicals: reactive nitrogen species, reactive oxygen species, transition metal ions, and the vascular system. Pharmacol. Res. **13**, 649–662
7 Sohal, R. S. and Weindruch, R. (1996) Oxidative stress, caloric restriction, and aging. Science **273**, 59–63
8 Sun, Y., Oberley, L. W., Oberley, T. D., Elwell, J. H. and Sierra-Rivera, E. (1993) Lowered antioxidant enzymes in spontaneously transformed embryonic mouse liver cells in culture. Carcinogenesis **14**, 1457–1463
9 Li, J.-J., Oberley, L. W., St. Clair, D. K., Ridnour, L. A. and Oberley, T. D. (1995) Phenotypic changes induced in human breast cancer cells by overexpression of manganese-containing superoxide dismutase. Oncogene **10**, 1989–2000
10 Asikainen, T. M., Huang, T.-T., Sariola, H., Levanen, A.-L., Carlson, E., Lapatto, R., Epstein, C. J. and Raivio, K. O. (1999) The effect of hyperoxia and N-acetylcysteine on the lungs of neonatal manganese superoxide dismutase knockout mice. Free Radical Biol. Med. **27**, S31
11 Kinnula, V. L., Pietarinen-Runtti, P., Raivio, K., Kahlos, K., Pelin, K., Mattson, K. and Linnainmaa, K. (1996) Manganese superoxide dismutase in human pleural mesothelioma cell lines. Free Radical Biol. Med. **21**, 527–532
12 Radi, R., Thomson, L., Rubbo, H. and Prodanov, E. (1991) Cytochrome *c*-catalyzed oxidation of organic molecules by hydrogen peroxide. Arch. Biochem. Biophys. **288**, 112–117
13 Radi, R., Turrens, J. F. and Freeman, B. A. (1991) Cytochrome *c*-catalyzed membrane lipid peroxidation by hydrogen peroxide. Arch. Biochem. Biophys. **288**, 118–125
14 Maiorino, M., Ursini, F. and Cadenas, E. (1994) Reactivity of metmyoglobin towards phospholipid hydroperoxides. Free Radical Biol. Med. **16**, 661–667
15 Radi, R., Sims, S., Cassina, A. and Turrens, J. F. (1993) Roles of catalase and cytochrome *c* in hydroperoxide-dependent lipid peroxidation and chemiluminescence in rat heart and kidney mitochondria. Free Radical Biol. Med. **15**, 653–659
16 Radi, R., Bush, K. M. and Freeman, B. A. (1993) The role of cytochrome-*c* and mitochondrial catalase in hydroperoxide-induced heart mitochondrial lipid peroxidation. Arch. Biochem. Biophys. **300**, 409–415
17 Barr, D. P., Gunther, M. R., Deterding, L. J., Tomer, K. B. and Mason, R. P. (1996) ESR spin-trapping of a protein-derived tyrosyl radical from the reaction of cytochrome *c* with hydrogen peroxide. J. Biol. Chem. **271**, 15498–15503
18 Gunther, M. R., Tschirret-Guth, R. A., Witkowska, H. E., Fann, Y. C., Barr, D. P., Ortiz de Montellano, P. R. and Mason, R. P. (1998) Site-specific spin trapping of tyrosine radicals in the oxidation of metmyoglobin by hydrogen peroxide. Biochem. J. **330**, 1293–1299
19 Bose-Basu, B., DeRose, E. F., Chen, Y.-R., Levy, L. A., Mason, R. P. and London, R. E. (2001) Protein NMR spin trapping with [methyl-$^{13}C_3$]MNP; application to the tyrosyl radical of equine myoglobin. Free Radical Biol. Med. **31**, 383–390
20 Pedersen, J. A. and Torssell, K. (1971) Electron spin resonance and nuclear magnetic resonance spectra of sterically hindered aromatic nitroxide radicals. Synthesis of stable nitroxide radicals. Acta Chem. Scand. **25**, 3151–3162
21 Makino, K. and Hatano, H. (1979) Separation and characterization of short-lived radicals in DL-methionine aqueous solution by high speed liquid chromatograph equipped with ESR spectrometer. Chem. Lett. 119–122
22 Makino, K., Moriya, F. and Hatano, H. (1985) Separation of free radicals by high-performance liquid chromatography with electron spin resonance detection. J. Chromatogr. **332**, 71–106
23 Iwahashi, H., Ikeda, A., Negoro, Y. and Kido, R. (1986) Detection of radical species in haematin-catalysed retinoic acid 5,6-epoxidation by using HPLC-EPR spectrometry. Biochem. J. **236**, 509–514
24 Iwahashi, H., Deterding, L. J., Parker, C. E., Mason, R. P. and Tomer, K. B. (1996) Identification of radical adducts formed in the reactions of unsaturated fatty acids with soybean lipoxygenase using continuous flow fast atom bombardment with tandem mass spectrometry. Free Radical Res. **25**, 255–274
25 Iwahashi, H., Parker, C. E., Tomer, K. B. and Mason, R. P. (1992) Detection of the ethyl- and pentyl-radical adducts of α-(4-pyridyl 1-oxide)-*N*-*tert*-butylnitrone in rat-liver microsomes treated with ADP, NADPH, and ferric chloride. Free Radical Res. Commun. **16**, 295–301
26 Iwahashi, H., Parker, C. E., Mason, R. P. and Tomer, K. B. (1992) Combined liquid chromatography/electron paramagnetic resonance spectrometry/electrospray ionization mass spectrometry for radical identification. Anal. Chem. **64**, 2244–2252
27 Iwahashi, H., Parker, C. E., Mason, R. P. and Tomer, K. B. (1991) Radical adducts of nitrosobenzene and 2-methyl-2-nitrosopropane with 12,13-epoxylinoleic acid radical, 12,13-epoxylinolenic acid radical and 14,15-epoxyarachidonic acid radical. Identification by HPLC-EPR and liquid chromatography-thermospray-MS. Biochem. J. **276**, 447–453
28 Iwahashi, H., Albro, P. W., McGown, S. R., Tomer, K. B. and Mason, R. P. (1991) Isolation and identification of α-(4-pyridyl 1-oxide)-*N*-*tert*-butylnitrone radical adducts formed by the decomposition of the hydroperoxides of linoleic acid, linolenic acid, and arachidonic acid by soybean lipoxygenase. Arch. Biochem. Biophys. **285**, 172–180
29 Duling, D. R. (1994) Simulation of multiple isotropic spin trap EPR spectra. J. Magn. Reson. Ser. B. **104**, 105–110
30 Borchers, C., Parker, C. E., Deterding, L. J. and Tomer, K. B. (1999) Preliminary comparison of precursor scans and liquid chromatography-tandem mass spectrometry on a hybrid quadrupole time-of-flight mass spectrometer. J. Chromatogr. A. **854**, 119–130
31 Deterding, L. J., Moseley, M. A., Tomer, K. B. and Jorgenson, J. W. (1989) Coaxial continuous-flow fast atom bombardment in conjunction with tandem mass spectrometry for the analysis of biomolecules. Anal. Chem. **61**, 2504–2511
32 Briere, R., Chapelet-Letourneux, G., Lemaire, H. and Rassat, A. (971) Nitroxydes. XXXV. Etude de l'interaction hyperfine electron-carbone-13; radicaux nitroxydes selectivement marques en α de l'azote. Mol. Phys. **20**, 211–224
33 McCormick, M. L., Gaut, J. P., Lin, T. S., Britigan, B. E., Buettner, G. R. and Heinecke, J. W. (1998) Electron paramagnetic resonance detection of free tyrosyl radical generated by myeloperoxidase, lactoperoxidase, and horseradish peroxidase. J. Biol. Chem. **273**, 32030–32037
34 Dole, F., Diner, B. A., Hoganson, C. W., Babcock, G. T. and Britt, R. D. (1997) Determination of the electron spin density on the phenolic oxygen of the tyrosyl radical of photosystem II. J. Am. Chem. Soc. **119**, 11 540–11 541
35 Suehiro, T., Kamimori, M., Sakuragi, H., Yoshida, M. and Tokumaru, K. (1976) Spin trapping of benzoyloxycyclohexadienyl radicals by 2,3,5,6-*tetra*-methylnitrosobenzene (nitrosodurene) in the decomposition of dibenzoyl peroxide in benzene. Bull. Chem. Soc. Jpn. **49**, 2594–2595
36 Kamimori, M., Sakuragi, H., Suehiro, T., Tokumaru, K. and Yoshida, M. (1977) Spin trapping of aryl and arylcyclohexadienyl radicals by *N*-*t*-butyl-α-phenylnitrone (*N*-benzylidene-*t*-butylamine oxide) and α,*N*-diphenylnitrone (*N*-benzylideneaniline oxide). Bull. Chem. Soc. Jpn. **50**, 1195–1200
37 Torssell, K. (1970) Investigation of radical intermediates in organic reactions by use of nitroso compounds as scavengers. The nitroxide method. Tetrahedron **26**, 2759–2773
38 Chignell, C. F. and Sik, R. H. (1989) Spectroscopic studies of cutaneous photosensitizing agents-XIV. The spin trapping of free radicals formed during the photolysis of halogenated salicylanilide antibacterial agents. Photochem. Photobiol. **50**, 287–295

Received 27 November 2001/8 January 2002; accepted 4 February 2002